

Supporting Information

© Wiley-VCH 2012

69451 Weinheim, Germany

Solid-State NMR Spectroscopy of Functional Amyloid from a Fungal Hydrophobin: A Well-Ordered β -Sheet Core Amidst Structural Heterogeneity**

Vanessa K. Morris, Rasmus Linser, Karyn L. Wilde, Anthony P. Duff, Margaret Sunde, and Ann H. Kwan**

anie_201205625_sm_miscellaneous_information.pdf

Supplementary Information

Circular dichroism (CD) spectropolarimetry:

CD spectra were recorded on unlabelled EAS $_{\Delta 15}$ in solution and as rodlets as reported previously.^[1] The concentration of EAS $_{\Delta 15}$ was 5 μM for the solution spectrum. For the solid-phase spectrum, a dried down 10- μL drop at a protein concentration of 60 μM was used.

Negative stain transmission electron microscopy:

A sample of EAS $_{\Delta 15}$ was prepared from lyophilised protein at a concentration of 0.1 mg/ml in 20% ethanol. A drop of EAS $_{\Delta 15}$ solution (20 μl) was pipetted onto a sheet of ParafilmTM and incubated for 10 min at room temperature, to allow the formation of a rodlet monolayer on the drop surface. Copper grids (200 mesh from ProSciTech, Australia) were prepared with pioloform plastic films and subsequently carbon-coated. Protein was transferred by floating the grid on the surface of the EAS $_{\Delta 15}$ -containing drop for 30 s. The excess liquid was removed by briefly touching the edge of the grid with filter paper. The grid was then washed three times with filtered water and stained by floating on a drop of 2% uranyl acetate for 10 min. Excess stain was removed by touching the edge of the grid with filter paper and the grid was then examined in a Phillips CM12 electron microscope operating at 120 kV, equipped with an iTEM digital imaging system.

Sample preparation:

EAS $_{\Delta 15}$ was previously expressed recombinantly in *Escherichia coli* using the pHUE vector.^[1b,2] To enable efficient expression of deuterated protein, the His₆-Ubiquitin-EAS $_{\Delta 15}$ coding sequence was subcloned into the pET28a vector.^[3] To generate samples with minimal background protonation, ²H,¹³C,¹⁵N-labelled EAS $_{\Delta 15}$ was cultured in minimal medium based on “ModC1”,^[4] using 100% D₂O, with ²H,¹³C(d7)-labelled glucose (10 g/L) as the sole carbon source and ¹⁵N-ammonium chloride (a total of 5.2 g/L; with half of this amount added at induction) as the sole nitrogen source. Control of pH was achieved by the addition of sodium deuterioxide, NaOD. EAS $_{\Delta 15}$ was purified

as described previously.^[1] The purified and fully-folded protein was then exchanged into 25% H₂O/D₂O and exchange of all amides was confirmed using solution ¹⁵N/¹H-HSQC spectra.

Rodlet formation was achieved by agitation of the soluble protein at a concentration of 130 μM in aqueous solution to maximize air-water interfaces.^[1] NaN₃ (0.03%) was added to the protein samples to inhibit bacterial growth. Protein rodlets were spun at increasing speeds (up to 5000 ×g) into a home-made funnel mounted on top of a 2.5 mm solid-state rotor. The rodlets were further compacted inside the rotor by centrifugation at 10000 ×g for 30 min. The filled rotor was then spun at 15 kHz in the stator of the spectrometer for 30 min, and the spin-and-pack process was repeated three times to fill the rotor as much as possible.

Solid-state NMR:

The samples were packed using a spacer formed from compressed Teflon[®] tape in the bottom of the rotor and a long cap to confine the sample volume to the central cavity. All spectra were recorded at 700 MHz proton Larmor frequency with a 2.5-mm triple-resonance probe.

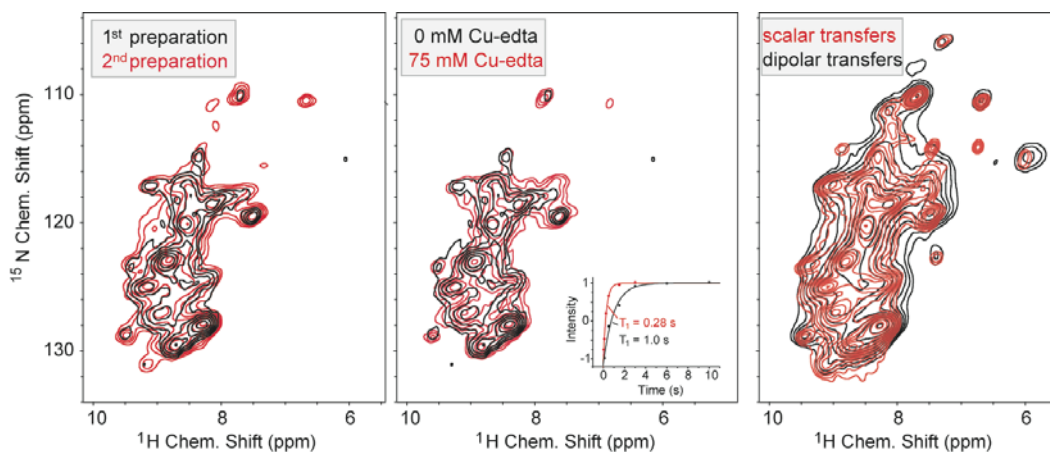
All ¹⁵N/¹H-correlations were recorded on ²H,¹³C,¹⁵N-labelled EAS_{Δ15} with a back exchange of labile protons in 25%:75% H₂O:D₂O. Paramagnetic Relaxation Enhancement (PRE)^[5] was used to overcome sensitivity limits posed by long relaxation delays. Rather than precipitating protein in a buffer containing paramagnetic ions, as was done in previous studies, 3 μL of 75 mM [Cu(edta)]²⁻ was simply added posteriorly into the rotor containing previously prepared EAS_{Δ15} rodlets. The Cu^{II} solution was replaced by a fresh aliquot after 30 min of incubation. Supplementary Figure 1B shows a comparison of spectra obtained from EAS_{Δ15} rodlets before and after Cu^{II} doping together with their ¹H T₁ relaxation profiles. Longitudinal relaxation times T₁, as compared with micro-crystalline preparations, were already quite short even without paramagnetic doping. The H^N bulk longitudinal relaxation time obtained after doping decreased to 0.28 s from 1 s, hence a recycled delay of 0.4 s was chosen for all subsequent

experiments. Significant chemical shift changes upon doping were not observed. These are not expected if the paramagnetic chelate undergoes stochastic displacement rather than specific binding to single amino acids.^[5a]

All $^{15}\text{N}/^1\text{H}$ spectra were recorded on a ~ 5 -mg sample at 25 kHz MAS at a temperature of ~ 15 °C for approximately 15 h each using a simplified Mississippi^[6] (dipolar correlations) or an HSQC pulse scheme (scalar correlations). H/N correlations were processed using a squared sine bell with a 60° and 90° phase shift in the ^1H and ^{15}N dimension, respectively. Zero filling was carried out to 8 k and 4 k points in the direct and indirect dimension, respectively.

Although an overall sample heterogeneity is apparent, the same distribution of conformational states is represented by successive sample preparations of deuterated protein (Supplementary Figure 1A) and is not altered by the inclusion of Cu^{II} -edta chelate (Supplementary Figure 1B).

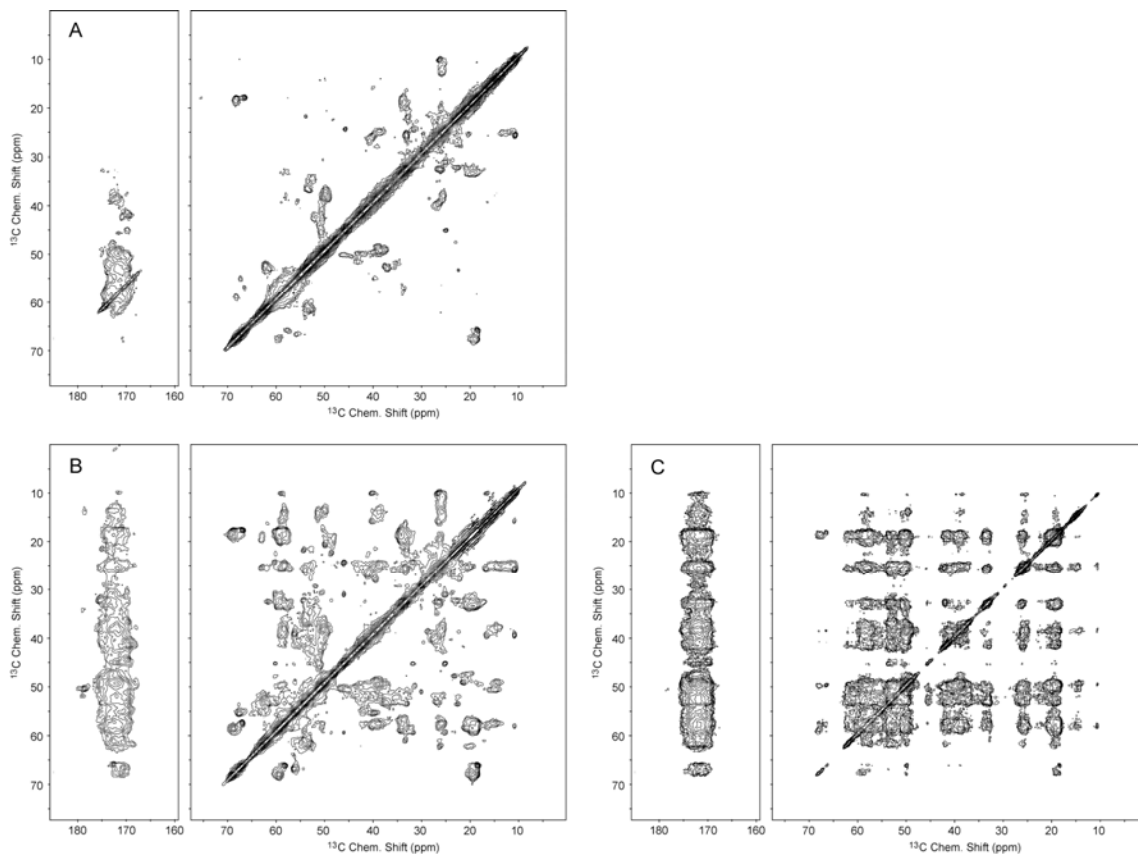
$^{15}\text{N}/^1\text{H}$ -correlation spectra were recorded via both scalar and dipolar transfers (Supplementary Figure 1C). The only resonances that are absent in the spectra recorded using dipolar coupling-based transfers but present in scalar-coupling experiments are exclusively side chain amide peaks. With dipolar-based Cross Polarization (in contrast to scalar transfers) being largely affected by motion-modulated dipolar coupling tensors, we can exclude intermediate to fast-time scale motion to be significant in the regions displaying defined peaks.



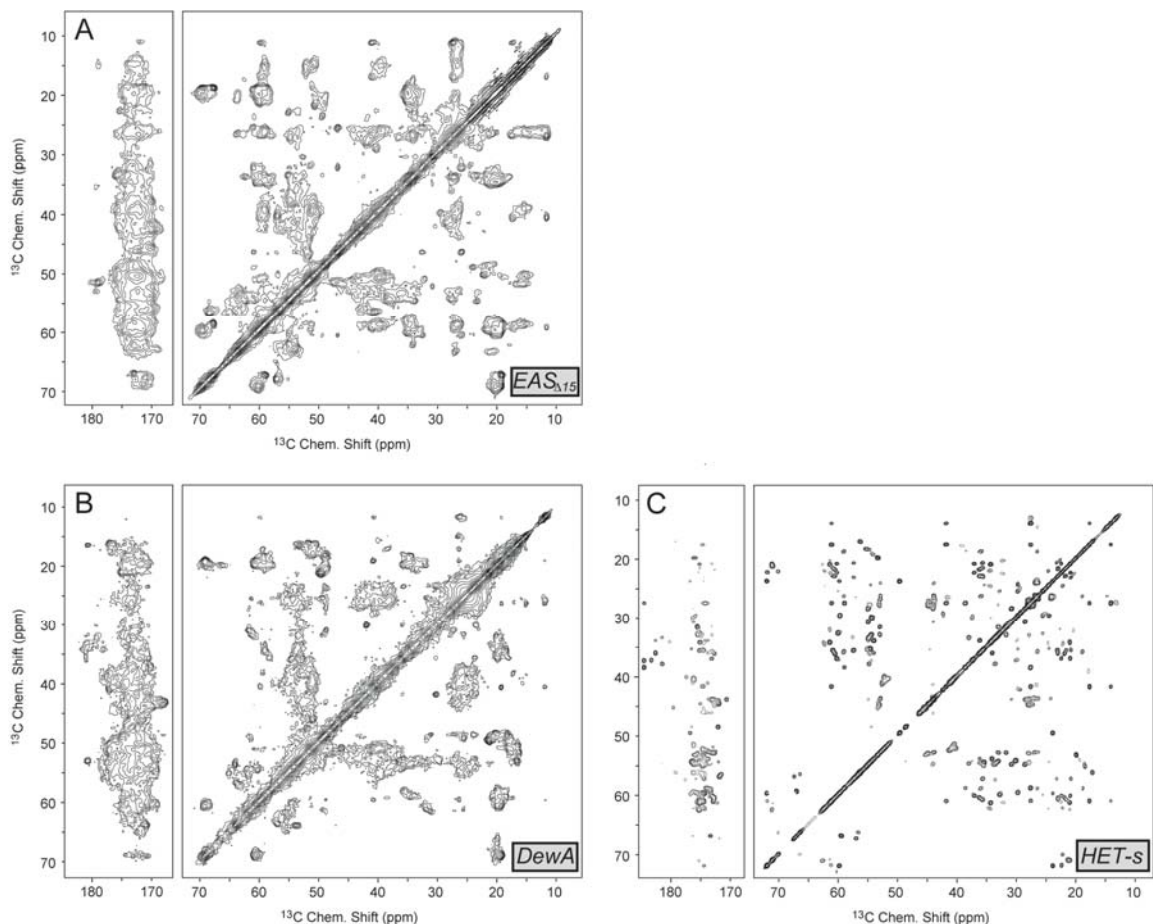
Supplementary Figure 1: **A)** Comparison of two rodlet preparations showing reproducibility of spectra; both spectra were recorded without paramagnetic doping. **B)** Comparison of the first rodlet preparation before (black) and after (red) paramagnetic doping with 75 mM $[\text{Cu}(\text{edta})]^{2-}$. Paramagnetic relaxation enhancement provides longitudinal relaxation times of less than 0.3 s. **C)** Comparison between $^{15}\text{N}/^1\text{H}$ correlation spectra recorded using scalar and dipolar transfers, depicted in red and black, respectively. Sample amounts used for spectra shown in A and B were only on the order of 2 mg each.

As in the case of $\text{A}\beta$ fibrils,^[6b] slow internal dynamics or chemical exchange processes seem to have a detrimental effect on coherence lifetimes, which are important for scalar transfers, particularly for heteronuclear magnetization transfers between low- γ nuclei such as ^{15}N and ^{13}C , which have small scalar coupling constants. Hence, this significantly shifts the balance between performance of scalar and dipolar transfers for HNC triple-resonance experiments towards the latter (data not shown).

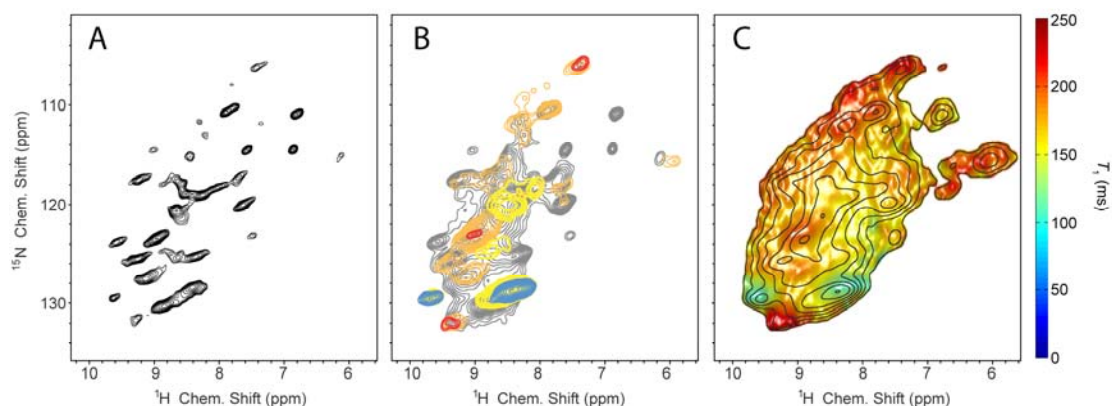
All $^{13}\text{C}/^{13}\text{C}$ correlations and NCACX experiments (data not shown) were recorded on a ^{13}C , ^{15}N -labelled sample of $\text{EAS}_{\Delta 15}$ at ~ 25 °C, using ~ 5 mg of rodlets and a rotor frequency of 15 kHz. The spectral width was set to 284 ppm, decoupling to 86 kHz using SPINAL-64, and the acquisition times typically set to 12 ms. Spectra were processed using $16\text{ k} \times 4\text{ k}$ points and with 30 Hz exponential line-broadening in both dimensions.



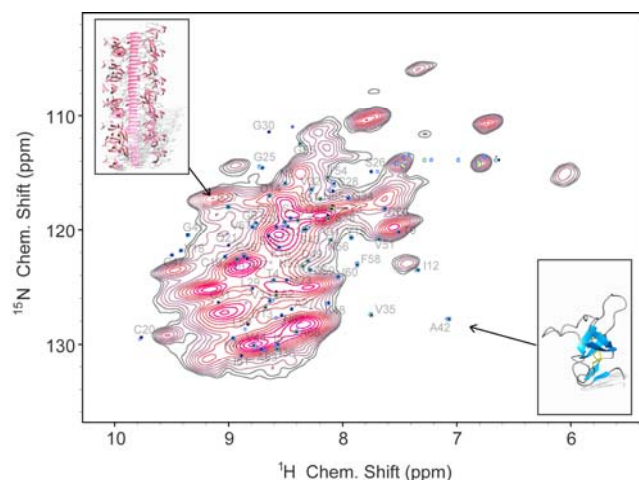
Supplementary Figure 2: **A)** Mixing via PDSD^[7] for 5 ms. This experiment was recorded with 10 kHz MAS in 17 h, using 32 scans and 1300 increments resembling 13 ms $t_{1\text{max}}$. **B)** Mixing via DARR^[8] for 50 ms. The spectrum was recorded in 29 h, using 64 scans and 800 increments of the indirect acquisition and 8 ms $t_{1\text{max}}$. **C)** Mixing via DARR for 500 ms. The spectrum was recorded in 1.5 d, using 64 scans and 1200 increments resulting in 12 ms $t_{1\text{max}}$.



Supplementary Figure 3: Comparison between **A**) a rodlet preparation of the hydrophobin EAS Δ_{15} , **B**) a rodlet preparation of DewA, a hydrophobin found in the *A. nidulans* spore wall and **C**) the fungal HET-s (218–289), courtesy of Prof. Beat Meier^[9]. The spectra were recorded under comparable sample conditions using parameters as described above with 50 ms DARR mixing for EAS Δ_{15} and DewA. The spectra of EAS Δ_{15} and DewA display similar features (*e.g.*, broad signals), indicating that large amounts of structural heterogeneity coexist with structurally conserved residues in both rodlet samples. Please note that DewA has a monomer size of 11.4 kDa, which is larger than EAS Δ_{15} and HET-s (218–289). The HET-s (218–289) spectrum was recorded at 850 MHz at a temperature of ~ 3 °C and a rotor frequency of 19 kHz with 100 kHz SPINAL-64 decoupling and a DARR mixing time of 100 ms.



Supplementary Figure 4: **A)** Scalar-based (HSQC-type) $^{15}\text{N}/^1\text{H}$ correlation as shown in Figure 1G of the main manuscript, apodized severely with a squared sine bell phase shifted by 45° in both the direct and the indirect dimension. **B)** ^1H T_1 -edited $^{15}\text{N}/^1\text{H}$ correlations as obtained for 2D inversion-recovery experiments using 80 and 120 ms inversion delays, overlaid on a standard scalar $^{15}\text{N}/^1\text{H}$ correlation (grey). Fast (yellow) and very fast (blue) relaxing spectral contributions are the ones which have inverted their sign after delays of 120 and 80 ms, respectively. Slowly (orange) and very slowly relaxing signals (red) have not changed their sign even after 80 and 120 ms, respectively. Quantitative residue-resolved T_1 determination is not feasible due to peak overlap and unclear peak assignment. **C)** ^1H T_1 -edited $^{15}\text{N}/^1\text{H}$ correlation showing T_1 values extracted from consecutive inversion-recovery experiments recorded using delays of 0, 30, 80, 120, 150 and 350 ms. The data were fitted using a grid of 64×64 points in Sparky^[10] and presented using a Delauny-triangulation procedure using Matlab.^[11] Peaks with longer T_1 values (indicative of structured regions) display a good match to new peaks in the rodlet state with chemical shifts far from random coil values (Supplementary Figure 5).



Supplementary Figure 5: Overlay of rodlet (solid-state) $^{15}\text{N}/^1\text{H}$ correlation (pink) and solution-state $^{15}\text{N}/^1\text{H}$ -HSQC (blue) as shown in Figure 1 in the Main Text.

Solution NMR:

Solution NMR spectra were recorded on a 800 MHz spectrometer at 25 °C at pH 3.0 from a 300 μ M sample in a 5-mm Shigemi tube. The maximum evolution time in the direct and indirect dimension was set to 110 ms and 50 ms, respectively. Apodization typically employed squared sine bell multiplication with a 70° phase shift in both dimensions. The $^{15}\text{N}/^1\text{H}$ -HSQC spectrum in Figure 1F of the Main Text and Supplementary Figure 5 was recorded in 5 min using 1 scan.

Surface contact angle of water droplets:

Octadecyltrichlorosilane (OTS) was deposited onto silicon wafers to make a uniform and hydrophobic surface. EAS $_{\Delta 15}$ rodlets were then coated on OTS-treated silicon wafers. The contact angle of water droplets will depend on the hydrophobicity of the surface; the more hydrophobic a surface is, the larger is the contact angle due to repulsion between water molecules and the hydrophobic surface. Therefore, flatter drops indicate the surface has become more hydrophilic.

References:

- [1] a) A. H. Kwan, I. Macindoe, P. V. Vukasin, V. K. Morris, I. Kass, R. Gupte, A. E. Mark, M. D. Templeton, J. P. Mackay, M. Sunde, *J. Mol. Biol.* **2008**, *382*, 708–20; b) I. Macindoe, A. H. Kwan, Q. Ren, V. K. Morris, W. Yang, J. P. Mackay, M. Sunde, *Proc. Natl. Acad. Sci. U.S.A.* **2012**, *109*, E804–11.
- [2] A. H. Y. Kwan, R. D. Winefield, M. Sunde, J. M. Matthews, R. G. Haverkamp, M. D. Templeton, J. P. Mackay, *Proc. Natl. Acad. Sci. U.S.A.* **2006**, *103*, 3621–6.
- [3] X. Chen, K. L. Wilde, H. Wang, V. Lake, P. J. Holden, A. P. J. Middelberg, L. He, A. P. Duff, *Food Bioprod. Process.* **2012**, *90*, 563–72.
- [4] A. P. Middelberg, B. K. O'Neill, I. D. L Bogle, M. A. Snoswell, *Biotechnol. Bioeng.* **1991**, *38*, 363–70.
- [5] a) R. Linser, V. Chevelkov, A. Diehl, B. Reif, *J. Magn. Reson.* **2007**, *189*, 209–16; b) N. P. Wickramasinghe, S. Parthasarathy, C. R. Jones, C. Bhardwaj, F. Long, M. Kotecha, S. Mehboob, L. W.-M. Fung, J. Past, A. Samoson, et al., *Nat. Methods* **2009**, *6*, 215–43.
- [6] a) D. H. Zhou, C. M. Rienstra, *J. Magn. Reson.* **2008**, *192*, 167–72; b) R. Linser, M. Dasari, M. Hiller, V. Higman, U. Fink, J.-M. Lopez del Amo, S. Markovic, L. Handel, B. Kessler, P. Schmieder, et al., *Angew. Chem., Int. Ed.* **2011**, *50*, 4508–12.
- [7] N. M. Szeverenyi, M. J. Sullivan, G. E. Maciel, *J. Magn. Reson.* **1982**, *47*, 462–75.
- [8] K. Takegoshi, S. Nakamura, T. Terao, *Chem. Phys. Lett.* **2001**, *344*, 631–7.
- [9] M. A. Stringer, W. E. Timberlake, *Mol. Microbiol.* **1995**, *16*, 33–44.
- [10] T. D. Goddard, D. G. Kneller, *SPARKY 3, University of California, San Francisco* **2004**.
- [11] Matlab, *The MathWorks, Inc.* **R2011b**.